Smart Materials and Devices

Science Exploration

Open Access Article

Load-responsive control of electrochromic windows for commercial buildings: Global cooling benefits and climate-dependent energy trade-offs

Pin-Yu Chen, Xinyi Tian, Yi Long*

Department of Electronic Engineering, The Chinese University of Hong Kong, Hong Kong SAR, China.

***Correspondence to:** Yi Long, Department of Electronic Engineering, The Chinese University of Hong Kong, Hong Kong SAR, China. E-mail: yilong@ee.cuhk.edu.hk

Received: August 14, 2026 **Accepted:** September 28, 2026 **Published:** October 08, 2026

Cite this article: Chen PY, Tian X, Long Y. Load-responsive control of electrochromic windows for commercial buildings: Global cooling benefits and climate-dependent energy trade-offs. Smart Mater Devices. 2027;3:202657. https://doi.org/10.70401/smd.2026.0053

Abstract

Electrochromic (EC) glazing can regulate solar heat gain, but the control signal affects the balance between cooling and heating energy use. This study compares the Load strategy, which uses predicted sensible load, with the fixed temperature-based T24 strategy, which uses a 24 °C upper switching threshold. Both strategies were implemented through the EnergyPlus Energy Management System (EMS) under identical building, heating, ventilation, and air-conditioning (HVAC), thermostat, weather, and EC glazing conditions across 384 worldwide EnergyPlus Weather (EPW) records. EC (Load) reduced cooling electricity across most climates but increased heating gas use, with larger penalties in colder regions. The resulting annual energy-use intensity (EUI) was 146.54 kWh m^{-2} $year^{-1}$ for EC (Load) and 145.23 kWh m^{-2} $year^{-1}$ for EC (T24), while the carbon-equivalent response varied geographically because of the competing electricity and heating effects. These results indicate that the Load strategy primarily redistributes energy use between cooling and heating rather than providing a universal annual-energy advantage, thereby demonstrating the climate-dependent energy trade-offs associated with this strategy.

Keywords: Electrochromic glazing, smart windows, EnergyPlus, load-responsive control, temperature-based control, climate-dependent energy performance

1. Introduction

1.1 Smart windows and electrochromic glazing

Smart windows have attracted increasing attention as adaptive building-envelope technologies because they can dynamically regulate solar radiation and visible light in response to changing environmental and operating conditions[1]. Among the various smart window technologies, electrochromic (EC), thermochromic, photochromic, and mechanochromic systems have been extensively investigated for improving building energy performance[2]. EC glazing is particularly attractive because its optical properties can be actively adjusted, allowing solar heat gain to be modulated according to building requirements[3].

Recent advances have expanded the capabilities of EC smart windows beyond conventional visible-light modulation. Full-spectrum solar regulation and enhanced near-infrared modulation can improve control of both daylight and solar heat gain, while scalable and flexible device architectures support larger-area deployment[4-7]. Complementary building-level studies have combined experimentally characterized EC systems with annual energy and daylight simulations, large-scale testing, calibrated building models, and visual-comfort assessment across multiple climates[8-11]. Together, these studies highlight the importance of device-realistic inputs, experimental validation, climate, and visual comfort in building-scale EC assessment. However, the effect of changing only the EC switching signal on the cooling-heating balance under otherwise identical conditions and across a broad global climate dataset remains less clearly established.

Dynamic glazing is relevant to commercial buildings, where perimeter zones experience substantial variations in solar exposure, thermal loads, daylight availability, and glare throughout the day and across seasons[2,12]. Switching between clear and dark optical states allows EC glazing to respond to these changing conditions[3]. Conventional low-emissivity (Low-E) glazing, by comparison, has fixed optical properties and cannot provide the same dynamic modulation of solar heat gain[2].

© The Author(s) 2026. This is an Open Access article licensed under a Creative Commons Attribution 4.0 International License (https://creativecommons.org/licenses/by/4.0/), which permits unrestricted use, sharing, adaptation, distribution and reproduction in any medium or format, for any purpose, even commercially, as long as you give appropriate credit to the original author(s) and the source, provide a link to the Creative Commons license, and indicate if changes were made.

1.2 Why control logic matters

The operation of EC glazing depends on the signal used to trigger transitions between optical states. Previous studies have considered schedules, environmental variables, indoor conditions, and predictive approaches, with different control strategies producing different heating and cooling responses[13-16]. Control logic therefore affects not only when EC glazing switches, but also how solar gains are distributed between periods of cooling and heating demand.

Fixed temperature-based control offers a simple approach in which glazing states are selected according to predefined indoor temperature thresholds. The choice of threshold, however, changes the timing of dark-state operation. Earlier suppression of solar heat gain may reduce cooling demand while limiting solar gains that would otherwise contribute to space heating. A higher threshold retains those gains for longer but delays the cooling response[14,15]. The consequences of threshold selection are therefore closely tied to climate and the relative importance of cooling and heating.

Predicted thermal load provides an alternative control signal. Rather than waiting for zone air temperature to cross a fixed threshold, load-responsive control can use predicted heating and cooling requirements to determine the EC state[16]. In the present study, the Load strategy is a binary sign-based strategy that uses only the sign of the EnergyPlus-predicted sensible load. It does not use load magnitude, an optimization objective, a prediction horizon, or multi-step optimization. Predictive and model predictive control (MPC) approaches generally use forecasts and optimization procedures to determine the operation of EC glazing[17,18]. More recent studies have examined glare-predictive split-pane control[19], direct comparisons of rule-based, proportional-integral-derivative and model predictive control algorithms under consistent glazing representations[20], and rule-based versus model-based control of experimentally characterized dual-band EC glazing across multiple European climates[21]. These studies show that EC performance depends on the control objective, glazing representation, comfort constraints, and climate. In contrast, the Load strategy in this study directly uses the predicted sensible heating or cooling load as an Energy Management System (EMS) switching signal, without a rolling-horizon optimization procedure. It is therefore categorized as a load-responsive rule-based control strategy rather than a full MPC controller.

1.3 EMS implementation of the control strategies

EnergyPlus provides a built-in EMS for implementing customized control logic within whole-building simulations. In this study, EMS was used to compare two EC control strategies under otherwise identical building and glazing conditions.

The Load strategy uses the sign of predicted sensible heating and cooling loads to determine the EC state. Cooling demand triggers the dark state to reduce solar heat gain, whereas heating demand triggers the clear state to promote passive solar gain. The T24 strategy uses zone air temperature with a 24 °C upper switching threshold. Both strategies employ the same EC clear and dark states and the same heating, ventilation, and air-conditioning (HVAC) thermostat schedules. Their comparison therefore isolates the consequences of changing the control signal from zone air temperature to predicted sensible load.

1.4 Scope and contribution

This study compares the EC (Load) and EC (T24) cases across diverse climates using a large-office reference model. Building geometry, internal loads, HVAC systems, operating schedules, thermostat setpoints, weather conditions, and EC properties were held constant between the two cases. A fixed Low-E reference was also retained to place the annual performance of EC glazing in context.

The simulations cover 384 EnergyPlus Weather (EPW) records spanning 17 detailed American Society of Heating, Refrigerating and Air-Conditioning Engineers (ASHRAE) Standard 169-2020 climate-zone categories. Facility electricity, cooling electricity, heating gas, carbon equivalent, representative-climate temporal responses, and annual energy-use intensity (EUI) were examined. Building on recent experimental studies, calibrated building simulations, and comfort-oriented EC-control research, this study does not seek to validate a new EC product or develop a multivariable optimization controller. Instead, it provides a controlled and reproducible comparison of the Load and T24 strategies by isolating the effect of the switching signal under otherwise identical building and EC-glazing conditions across 384 EPW records. This design quantifies how control-signal choice redistributes cooling and heating energy across 17 climate-zone categories. A supplementary threshold-sensitivity analysis examines how the fixed temperature benchmark changes when the upper switching threshold is varied.

2. Methodology

2.1 Overall workflow

Figure 1 summarizes the simulation framework, EMS control strategies, and performance analysis. The simulation framework included the fixed Low-E reference and EC glazing represented by predefined clear and dark optical states. Two EMS-based strategies were applied to the EC glazing: T24, based on zone air temperature, and Load, based on predicted sensible heating and cooling loads. The EC properties and building conditions were identical between the two strategies.

Simulation outputs were examined using global spatial maps, ASHRAE climate-zone statistics, representative-climate temporal

heatmaps, and annual whole-building end-use decomposition. Together, these analyses resolve how the two control signals affect cooling, heating, and annual building performance. Figure 2 was prepared from post-processed EnergyPlus output data. Detailed source data and preparation procedures are provided in Section S3.5 and Table S4.

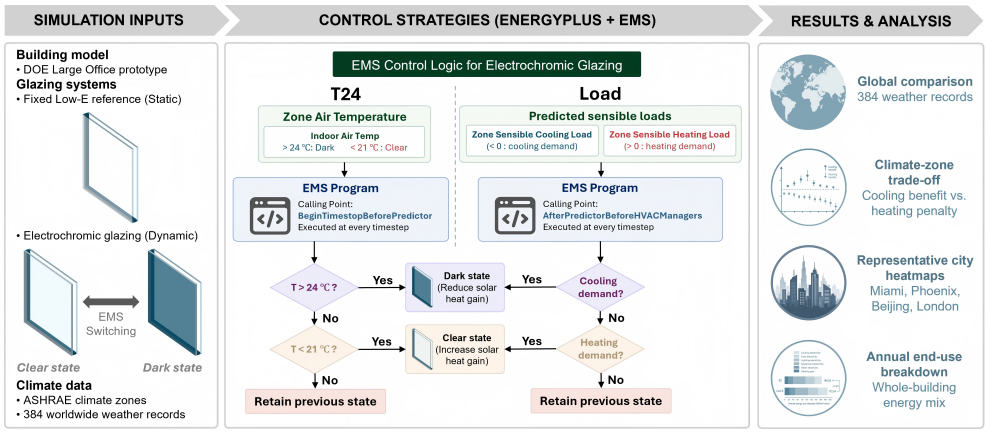


Figure 1. Overall simulation and analysis framework. EMS: Energy Management System; ASHRAE: American Society of Heating, Refrigerating and Air-Conditioning Engineers; DOE: U.S. Department of Energy.

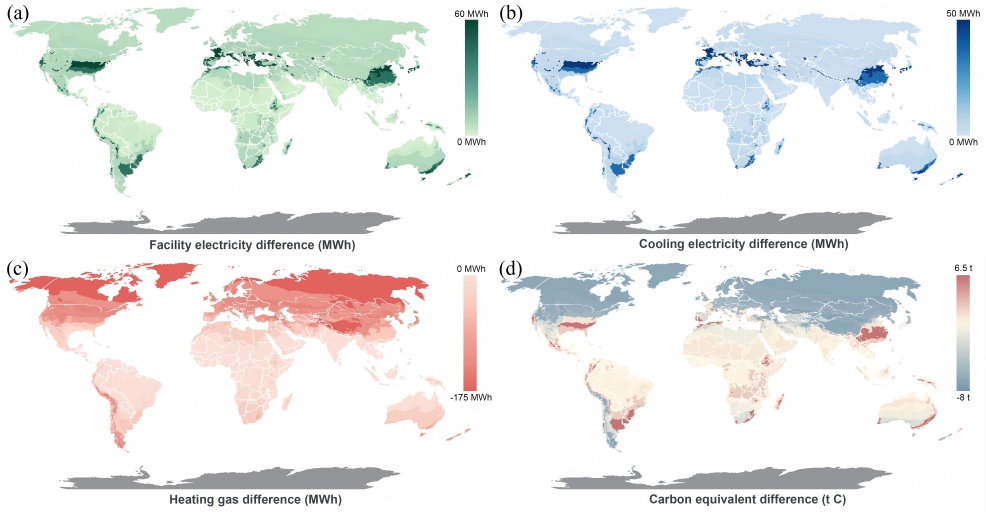


Figure 2. Differences between EC (T24) and EC (Load), based on 384 EPW records and averaged within 17 climate-zone categories. Differences are calculated as EC (T24)−EC (Load). Positive values indicate lower energy use or carbon-equivalent output under EC (Load). (a) Facility electricity; (b) Cooling electricity; (c) Heating gas; (d) Carbon equivalent. EC: electrochromic; EPW: EnergyPlus Weather.

2.2 Building prototype and simulation settings

The simulations were conducted using the U.S. Department of Energy (DOE) Commercial Reference Building Large Office prototype, which complies with ASHRAE Standard 90.1-2004[22]. The reference building is a 12-story office building with a basement and a total floor area of 46,320 m^2. The façade has a window-to-wall ratio of 38 %, with windows evenly distributed across the four cardinal orientations. The original DOE thermal zoning configuration was retained, including perimeter and core zones on the bottom, middle, and top floors.

The building was simulated in EnergyPlus version 9.1 using the default HVAC system and operating schedules specified in the DOE Reference Building. Detached shading devices, natural ventilation, and daylight-responsive lighting controls were excluded to isolate the influence of glazing control. The occupied heating and cooling setpoints were 21.0 °C and 24.0 °C, respectively, with setback temperatures of 15.6 °C and 26.7 °C during unoccupied periods. These thermostat schedules were identical in all cases. The 24 °C upper switching threshold used in T24 corresponded to the occupied cooling setpoint. However, the T24 EMS thresholds were fixed throughout the annual simulation and did not follow the occupied or unoccupied thermostat setbacks. Load relied on predicted sensible heating and cooling loads calculated relative to the same thermostat schedules. All simulations used six zone timesteps per hour, corresponding to a nominal 10-min zone timestep. The HVAC system timestep could be shorter when required for EnergyPlus convergence. The principal simulation settings are summarized in Section S3.2 and Table S1.

2.3 Glazing systems

The fixed Low-E reference was represented in EnergyPlus using a WindowMaterial:Glazing object with optical properties adopted from Table S5 in the Supporting Information of Wang *et al.*[23]. It remained fixed throughout the simulations without EMS switching.

The EC glazing was represented using the WindowMaterial:SimpleGlazingSystem object with predefined clear and dark optical states based on the performance range reported by DeForest *et al.*[13]. Both EC states were assigned the same U-factor of 1.9 W m^{-2} K^{-1} to isolate the influence of dynamic solar modulation. The clear state had a solar heat gain coefficient (SHGC) of 0.65 and visible transmittance (T_{vis}) of 0.68, whereas the dark state had an SHGC of 0.08 and T_{vis} of 0.10. The same EC constructions were used for all control cases.

The different EnergyPlus objects reflected the available property data. The EC states were defined using whole-window properties, whereas the Low-E reference was defined using fixed glazing-layer properties. Both window systems were compared under identical building, HVAC, schedule, weather, and boundary conditions, with EMS-controlled switching applied only to the EC window while the Low-E reference remained static. The EC model assumed idealized binary switching behavior. Switching electricity consumption, transition delay, hysteresis, optical degradation, and intermediate tint states were not considered. The simulations therefore isolated the effects of control-driven optical modulation rather than practical device-level switching characteristics. Complete Low-E source and construction details, together with the EC inputs and comparison basis, are provided in Section S3.3 and Table S2.

2.4 EMS-based EC control strategies

2.4.1 Temperature-based control

T24 used zone mean air temperature as the EMS sensing variable. The EC glazing switched to the dark state when the zone air temperature exceeded 24 °C and to the clear state when the temperature fell below 21 °C. Within the 21 °C to 24 °C deadband, the previous glazing state was retained. These fixed EMS thresholds were applied throughout the annual simulation. The 15.6 °C and 26.7 °C unoccupied HVAC thermostat setbacks remained active in the reference-building HVAC schedules but were not used as T24 switching thresholds.

The T24 EMS program was executed at the BeginTimestepBeforePredictor calling point because the strategy depends on current zone air temperature rather than predicted thermal loads. A secondary T23 strategy, implemented as the EC (T23) sensitivity case, used a 23 °C upper switching threshold. T23 was otherwise identical to T24, including the 21 °C lower threshold, EC states, building configuration, and HVAC settings. The threshold-sensitivity analysis is provided in Section S1, and the complete T24 EMS implementation is provided in Section S2.1.

2.4.2 Load strategy

Load used the predicted sensible cooling and heating loads of the 12 perimeter zones containing the actuated EC windows as EMS sensing variables. Under the sign convention used in the EMS implementation, a negative predicted cooling-load value indicates cooling demand, whereas a positive predicted heating-load value indicates heating demand.

The Load EMS program was executed at the AfterPredictorBeforeHVACManagers calling point, allowing predicted zone loads to be accessed after the predictor calculation and before the HVAC managers were executed. Cooling demand triggered the dark state to reduce solar heat gain, whereas heating demand triggered the clear state to promote passive solar heat gain. When neither cooling nor heating demand was predicted in a perimeter zone, the previous glazing state was retained. The glazing state was implemented by dynamically reassigning the window construction between the predefined clear and dark states. Because the predicted-load signal is available only after the predictor, it is calculated before the construction state newly assigned at this calling point is applied in subsequent simulation calculations. This creates a timing asymmetry relative to T24, which is evaluated before the predictor. This timing difference is acknowledged as a methodological limitation. The complete Load EMS implementation is provided in Section S2.2.

The Load strategy intentionally used only the sign of the predicted sensible cooling or heating load. Load magnitude was not used as a control input, and zone temperature, outdoor temperature, solar radiation, occupancy, and daylight availability were not directly included in the control logic. Although the strategy uses an EnergyPlus predicted sensible-load signal, it does not include an objective function, an optimization procedure, or a prediction horizon. This simplified design was selected to provide a transparent, low-complexity, and reproducible benchmark for comparing the Load and T24 strategies. A limitation of this approach is that it does not represent a comprehensive practical controller that responds to multiple environmental or operational variables. A detailed methodological comparison is provided in Section S3.6 and Table S5.

2.5 Global simulation matrix

We used a stratified set of 384 EPW records obtained from the Ladybug Tools EPW Map. Each record was assigned to one of the 17 detailed climate-zone categories defined by ASHRAE Standard 169-2020. The selection ensured at least 20 EPW records in each

category while maintaining broad geographic coverage across the climate-zone categories. Each EPW record was simulated for the principal cases EC (T24) and EC (Load), while the fixed Low-E reference was retained for whole-building energy comparison. EC (T23) was additionally simulated for the threshold-sensitivity analysis reported in Section S1. The complete file list and record-level metadata are provided in Data File S1.

The primary comparison between EC (T24) and EC (Load) used identical building geometry, HVAC systems, internal loads, operating schedules, thermostat setpoints, weather files, and EC properties. Differences between the two cases therefore reflect the change in control strategy rather than changes in glazing or building characteristics. For annual and global summaries, months 1–12 were first summed for each EPW record. Results were then averaged arithmetically within each of the 17 climate-zone categories. The 17 climate-zone means were subsequently averaged with equal weight.

Miami, Phoenix, Beijing, and London were selected as representative hot-humid, hot-dry, cold, and marine climates, respectively, for temporal analysis of the cooling-heating response.

2.6 Performance metrics

The comparison between EC (T24) and EC (Load) considered facility electricity, cooling electricity, heating gas, fan electricity, carbon equivalent, and annual whole-building EUI. Differences were calculated as the EC (T24) value minus the corresponding EC (Load) value. A positive difference therefore indicates a lower value under EC (Load), whereas a negative difference indicates a higher value under EC (Load). EUI was calculated from annual Electricity:Facility plus Heating:Gas, converted to kWh where necessary, and divided by the total floor area of 46,320 m^2. All reported EUI values were calculated from unrounded source data and rounded to two decimal places.

Cooling electricity and heating gas were examined separately to resolve changes in the cooling-heating balance. Facility electricity and carbon equivalent were used to assess the broader consequences of these changes, while annual EUI provided the whole-building comparison. Other electricity was defined as Electricity:Facility−(Cooling:Electricity + Fans:Electricity + InteriorLights:Electricity + InteriorEquipment:Electricity). This residual is already included in Electricity:Facility and was not added a second time. The fixed Low-E reference served as an additional reference for evaluating the annual energy performance of EC glazing.

Carbon-equivalent results were taken directly from the EnergyPlus output variable Carbon Equivalent:Facility. The EnergyPlus calculation can be expressed as:

$$CE = \sum_f E_f \left(EF_{CO_2,f} CF_{CO_2} + EF_{CH_4,f} CF_{CH_4} + EF_{N_2O,f} CF_{N_2O} \right) \times 10^{-3}$$

where E_f is the energy use of fuel f in MJ, EF is the fuel-specific emission factor in g MJ^{-1}, and CF is the carbon-equivalent conversion factor in kg C per kg of pollutant. The factor 10^{-3} converts pollutant mass from grams to kilograms. The conversion factors used by the model were 0.2727 kg C kg^{-1} CO_2, 6.2727 kg C kg^{-1} CH_4, and 80.7272 kg C kg^{-1} N_2O. Electricity emission factors were specific to the corresponding DOE climate-zone reference model and were not customized to the country or electricity grid of each EPW location, while natural-gas emission factors were uniform across the corresponding reference-building models. Therefore, the carbon-equivalent results reflect the DOE reference-model emission factors rather than the actual grid carbon intensity of each EPW location. The fixed Low-E reference, EC (Load), and EC (T24) cases retained the same factor definitions for each corresponding climate-zone model. The complete factor values are provided in Section S3.4 and Table S3.

For the climate-zone analysis in Figure 3, the EPW-record-level differences were grouped by detailed ASHRAE climate-zone category. The plotted symbols represent arithmetic means, and the error bars represent two-sided 95 % confidence intervals of the means. The calculation procedure is provided in Section S3.1.

3. Results and Discussion

3.1 Global differences between EC (T24) and EC (Load)

Figure 2 compares EC (T24) and EC (Load) by showing the mean differences for the 17 detailed climate-zone categories calculated from the 384 EPW records. Differences are reported as EC (T24)-EC (Load), so positive values indicate lower energy use or carbon-equivalent output under EC (Load).

Facility electricity was generally lower under EC (Load), although the magnitude varied geographically, as shown in Figure 2a. Cooling electricity exhibited the clearest response. Positive mean differences were observed for all 17 climate-zone categories in Figure 2b, showing that the Load strategy generally shifts EC operation toward lower cooling electricity consumption.

Heating moved in the opposite direction. Figure 2c shows predominantly negative heating gas differences, with larger penalties appearing in colder regions. Reduced solar heat gain is beneficial when cooling is required but can remove useful passive heat during heating periods. The carbon-equivalent response in Figure 2d is therefore spatially mixed, reflecting the competing effects of lower

electricity use and higher heating gas consumption.

3.2 Climate-zone cooling-heating trade-off

Figure 3 shows the EC (T24)−EC (Load) differences by detailed ASHRAE climate-zone category. Symbols represent arithmetic means of the EPW-record-level differences within each detailed category, with error bars indicating two-sided Student's t-based 95 % confidence intervals of the means, calculated as described in Section S3.1. The category-specific sample sizes are reported in Table S4 and Data File S1. Because the EPW records were selected using a stratified procedure rather than random independent sampling, the intervals are not interpreted as population-level uncertainty.

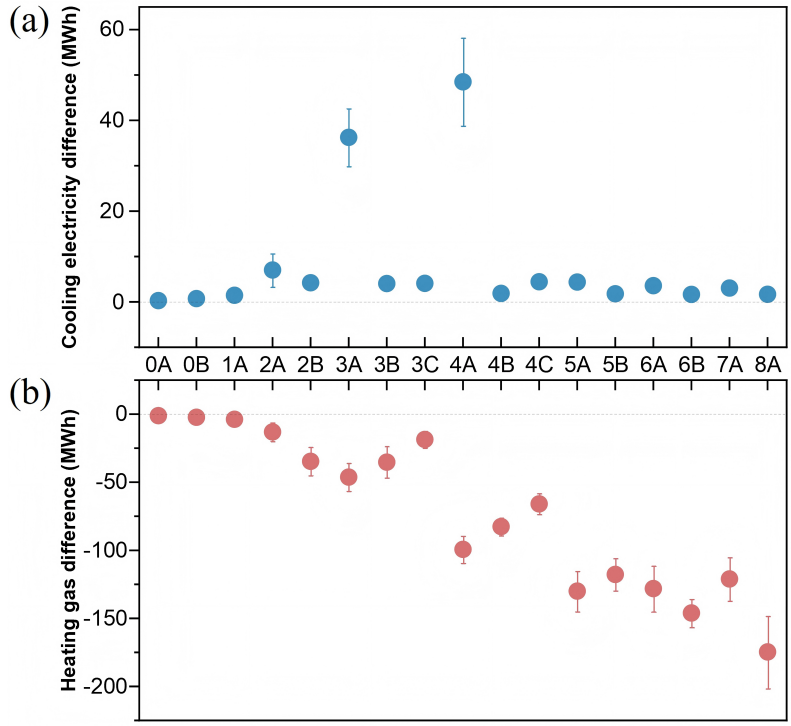


Figure 3. Climate-zone cooling-heating trade-off between EC (T24) and EC (Load). Symbols represent arithmetic means, and error bars indicate 95 % confidence intervals. Differences are calculated as EC (T24)−EC (Load). Positive values indicate lower energy use under EC (Load). (a) Cooling electricity difference; (b) Heating gas difference. EC: electrochromic.

Cooling electricity was lower under EC (Load) in all 17 detailed climate zones, as shown in Figure 3a. The largest mean differences occurred in 3A and 4A, while the reductions were smaller in colder zones with less annual cooling demand. The heating response differs markedly. In Figure 3b, heating gas differences are close to zero in warmer climates but become increasingly negative toward colder zones.

The two panels show that the EC (Load) case shifts the balance between cooling and heating rather than reducing both simultaneously. The cooling benefit remains evident across a broad range of climates, while the heating penalty grows as heating demand becomes more important. This divergence is reflected in the climate-dependent facility electricity and carbon-equivalent responses in Figure 2.

3.3 Representative-climate temporal response

Figure 4 examines the temporal structure of this trade-off in four representative climates. The heatmaps show monthly mean hourly differences calculated for each representative EPW location. For each month, values recorded at the same hour of day were averaged across all days in that month. Differences are calculated as EC (T24)−EC (Load), and the same color scale is used across the four cities for each metric.

Miami shows little heating response. In Figure 4a, cooling reductions occur mainly during daytime periods in winter and transitional months, while heating gas differences remain negligible throughout the year. Phoenix displays a more seasonal pattern in Figure 4b, with cooling reductions in winter, spring, and late autumn and a modest heating penalty during colder periods.

The separation between cooling and heating becomes clearer in the colder representative climates. Figure 4c shows that Beijing experiences cooling reductions mainly during spring and autumn daytime periods, together with pronounced heating penalties

during winter and transitional seasons. London, shown in Figure 4d, has moderate cooling reductions during spring and autumn and a less severe but more distributed heating penalty during the heating season.

The temporal results help explain why similar annual EUI values can conceal different control responses. Cooling reductions and heating penalties occur at different times of the year, and the latter becomes increasingly important as the climate shifts toward heating-dominated conditions.

3.4 Annual whole-building energy-use intensity

Figure 5 compares annual whole-building EUI and end-use composition for the fixed Low-E reference, EC (Load), and EC (T24). EC (Load) reduced EUI from 172.24 kWh m^{-2} $year^{-1}$ for the Low-E reference to 146.54 kWh m^{-2} $year^{-1}$, a reduction of 14.9 %. The changes were concentrated mainly in HVAC-related end uses, while lighting, equipment, and other electricity remained nearly unchanged.

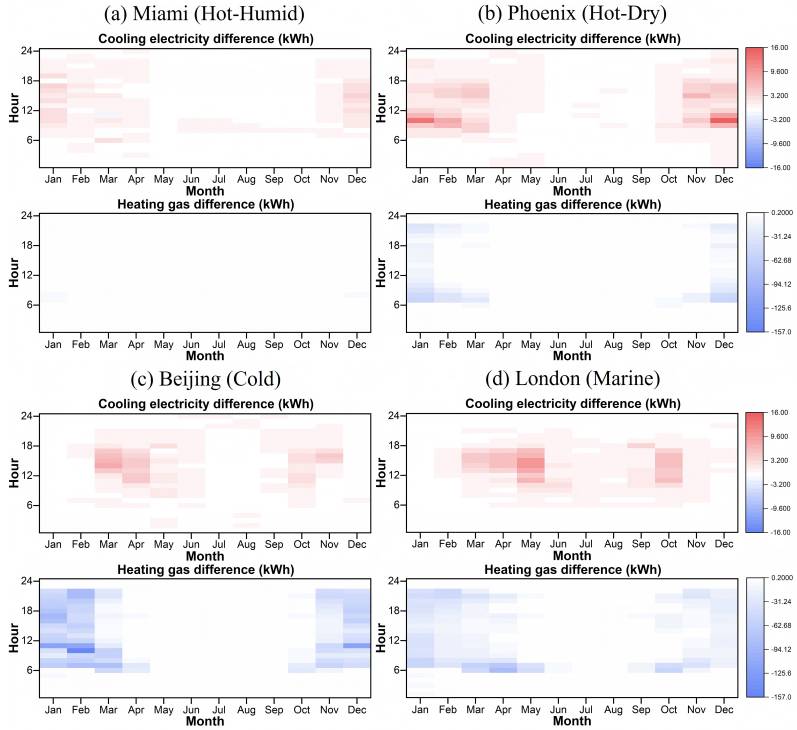


Figure 4. Monthly mean hourly cooling-heating trade-off between EC (T24) and EC (Load) under representative climates. Each cell shows the EC (T24)-EC (Load) difference averaged across all days of the corresponding month at the indicated hour of day. Positive values indicate lower values under EC (Load). (a) Miami (hot-humid); (b) Phoenix (hot-dry); (c) Beijing (cold); (d) London (marine). Rows show cooling electricity and heating gas differences. EC: electrochromic.

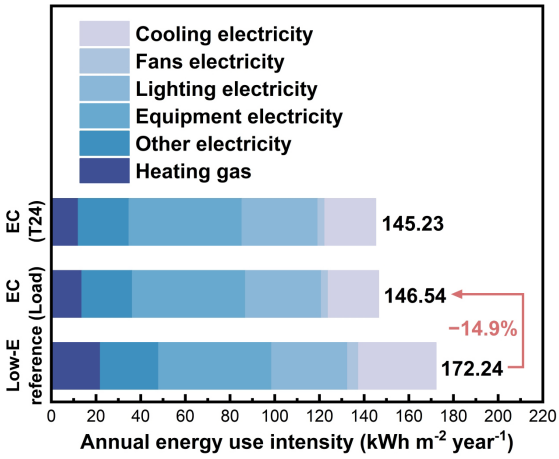


Figure 5. Annual whole-building EUI and end-use composition for the fixed Low-E reference, EC (Load), and EC (T24). Annual values were obtained by summing months 1-12 for each of 384 EPW records, averaging within 17 detailed climate-zone categories, and applying equal weight to the category means. EC: electrochromic; Low-E: low-emissivity; EUI: energy-use intensity; EPW: EnergyPlus Weather.

The distinction between EC (Load) and EC (T24) is much smaller at the whole-building level. Annual EUI was 146.54 kWh m^{-2} $year^{-1}$ for EC (Load) and 145.23 kWh m^{-2} $year^{-1}$ for EC (T24), a difference of 1.31 kWh m^{-2} $year^{-1}$, or approximately 0.9 %. Thus, the changes in cooling and heating end uses largely offset one another when aggregated over the year.

The threshold-sensitivity analysis in Figure S1 provides additional context for this comparison. Reducing the upper temperature threshold from 24 °C to 23 °C changes the cooling-heating balance and annual EUI across climate zones, showing that the performance of fixed temperature control depends on threshold selection. T24 is therefore used as a representative fixed temperature-based case rather than as a globally optimized threshold. The annual results should therefore be interpreted as a controlled simulation comparison rather than as predictions of long-term commercial EC performance. Recent experimental, calibrated, and *in situ* studies support the value of larger-scale testing and validation under realistic operating conditions[9,10,24], whereas practical deployment also depends on switching dynamics, sensing and control integration, optical stability, cycling durability, and occupant response[1,11]. These factors were outside the scope of the present study and require future field validation.

4. Conclusions

The EC (Load) and EC (T24) cases produced similar annual whole-building energy use, but they reached that outcome through different cooling and heating responses. EC (Load) reduced cooling electricity across most of the investigated climates, while increasing heating gas use. The heating penalty was small in warmer regions and became progressively larger toward colder climate zones.

These opposing responses largely cancel at the annual scale. EC (Load) produced an EUI of 146.54 kWh m^{-2} $year^{-1}$, compared with 145.23 kWh m^{-2} $year^{-1}$ for EC (T24). The choice of control signal therefore had a much stronger effect on the distribution of cooling and heating energy use than on total annual EUI. EC glazing itself remained advantageous relative to the fixed Low-E reference, with EC (Load) reducing annual EUI from 172.24 to 146.54 kWh m^{-2} $year^{-1}$, or 14.9 %. The T23 sensitivity case also confirmed that fixed temperature control is sensitive to the selected switching threshold.

Predicted sensible load is therefore useful for shifting EC operation toward lower cooling electricity consumption, but that shift should not be interpreted as an inherent annual energy advantage. In heating-dominated climates, the additional heating demand can offset the cooling reduction. Future control development should account for the magnitude of thermal demand and the availability of useful solar gain rather than relying only on the presence of predicted cooling or heating demand.

Supplementary materials

The supplementary material for this article is available at: Supplementary materials.

Declarations

Acknowledgements

The authors declare that OpenAI Codex was used solely for language polishing during manuscript preparation and revision. ChatGPT was used exclusively to generate three illustrative icons in the "Results & Analysis" section of Figure 1, including two schematic icons based on Figures 3 and 5 and one city skyline icon. All other figure elements were manually created by the authors. AI tools were not used for study design, data processing, data analysis, interpretation of results, or development of conclusions. All scientific content was produced and verified by the authors, who take full responsibility for the submitted work.

Authors contribution

Chen PY: Conceptualization, data curation, investigation, methodology, writing-original draft.
Tian X: Methodology.
Long Y: Funding acquisition, supervision, writing-review & editing.

Conflicts of interest

The authors declare no conflicts of interest.

Ethical approval

Not applicable.

Consent to participate

Not applicable.

Consent for publication

Not applicable.

Availability of data and materials

The data that support the findings of this study are available from the corresponding author upon reasonable request.

Funding

Long Y is thankful for funding support from the 2024 Shenzhen-Hong Kong-Macau Science and Technology Program (Category C) (Grant No. SGDX20230821094659005), the Innovation and Technology Fund (Grant No. ITS/221/23), and the Research Grants Council (Grant No. GRF2151330).

Copyright

© The Author(s) 2026.

References

1. Zhao F, Wang B, Huang B, Zhang W, Chen J, Liu L, et al. Inorganic electrochromic smart windows for advancing building energy efficiency. Nat Rev Clean Technol. 2025;1(6):396-412. [DOI]
2. Baetens R, Jelle BP, Gustavsen A. Properties, requirements and possibilities of smart windows for dynamic daylight and solar energy control in buildings: A state-of-the-art review. Sol Energy Mater Sol Cells. 2010;94(2):87-105. [DOI]
3. Shao Z, Huang A, Cao C, Ji X, Hu W, Luo H, et al. Tri-band electrochromic smart window for energy savings in buildings. Nat Sustain. 2024;7(6):796-803. [DOI]
4. Li H, Zhang J, Liu Y, Bai Z, Liang H, Hou C, et al. Scalable all-in-one electrochromic glazing for full-spectrum solar radiation management. Nat Sustain. 2026;9(6):910-920. [DOI]
5. Wu X, Bao B, Bai Z, Fan Q, Hou C, Zhang Q, et al. Heteroaromatic π-stacking engineered near-infrared absorption for highly stable near-zero transmittance electrochromic window. Nat Commun. 2025;16(1):9964. [DOI][PubMed][PMC]
6. Bao B, Hao Y, Wu X, Xiao R, Hou C, Li Y, et al. Redox-bipolar mesoporous two-dimensional covalent organic framework for multi-color electrochromism. Sci Adv. 2025;11(42):eaea1304. [DOI][PubMed][PMC]
7. Li R, Ma X, Li J, Cao J, Gao H, Li T, et al. Flexible and high-performance electrochromic devices enabled by self-assembled 2D TiO_2/MXene heterostructures. Nat Commun. 2021;12:1587. [DOI]
8. Cannavale A, Carlucci F, Pugliese M, Maiorano V, Ayr U, Fiorito F. Low-cost gel-polymer electrolytes for smart windows: Effects on yearly energy consumption and visual comfort. Energy Build. 2023;301:113705. [DOI]
9. Li Y, Shah KW, Li W, Xiong T. Experimental investigation on indoor thermal environment improvement and energy-saving of electrochromic window under Singapore's tropical climate. J Build Eng. 2023;73:106779. [DOI]
10. Teixeira H, Moret Rodrigues A, Aelenei D, Gomes MG. Simulation-based evaluation of the impact of an electrochromic glazing on the energy use and indoor comfort of an office room. Energies. 2024;17(9):2110. [DOI]
11. Jain S, Wienold J, Lagier M, Schueler A, Andersen M. Perceived glare from the Sun behind tinted glazing: Comparing blue *vs.* Color-neutral tints. Build Environ. 2023;234:110146. [DOI]
12. Tzempelikos A, Athienitis AK. The impact of shading design and control on building cooling and lighting demand. Sol Energy. 2007;81(3):369-382. [DOI]
13. DeForest N, Shehabi A, Selkowitz S, Milliron DJ. A comparative energy analysis of three electrochromic glazing technologies in commercial and residential buildings. Appl Energy. 2017;192:95-109. [DOI]
14. Assimakopoulos MN, Tsangrassoulis A, Santamouris M, Guarracino G. Comparing the energy performance of an electrochromic window under various control strategies. Build Environ. 2007;42(8):2829-2834. [DOI]
15. Lee ES, Tavil A. Energy and visual comfort performance of electrochromic windows with overhangs. Build Environ. 2007;42(6):2439-2449. [DOI]
16. Sun Y, Hao Y, Wang D, Wang W, Deng S, Qi H, et al. A predictive control strategy for electrochromic glazing to balance the visual and thermal environmental requirements: Approach and energy-saving potential assessment. Renew Energy. 2022;194:334-348. [DOI]
17. Isaia F, Fiorentini M, Serra V, Capozzoli A. Enhancing energy efficiency and comfort in buildings through model predictive control for dynamic façades with electrochromic glazing. J Build Eng. 2021;43:102535. [DOI]
18. Ganji Kheybari A, Steiner T, Liu S, Hoffmann S. Controlling switchable electrochromic glazing for energy savings, visual comfort and thermal comfort: A model predictive control. CivilEng. 2021;2(4):1019-1051. [DOI]
19. Sun Y, Li Y, Xu W, Wang W, Wei W, Zhang C. A glare predictive control strategy for split-pane electrochromic windows: Visual comfort and energy-saving assessment. Renew Energy. 2023;218:119259. [DOI]
20. Alkhatib H, Lemarchand P, Norton B, O'Sullivan DTJ. Comparative simulations of an electrochromic glazing and a roller blind as controlled by seven different algorithms. Results Eng. 2023;20:101467. [DOI]
21. Riganti M, Li Castri G, Serra V, Manca M, Favoino F. Energy saving potential of advanced dual-band electrochromic smart windows for office integration. Energy Build. 2025;327:115084. [DOI]

22. Deru M, Field K, Studer D, Benne K, Griffith B, Torcellini P, et al. U.S. Department of Energy commercial reference building models of the national building stock. Golden, CO: National Renewable Energy Laboratory; 2011 Feb. Report No.: NREL/TP-5500-46861. Available from: https://oasis.library.unlv.edu/renew_pubs/44/
23. Wang S, Jiang T, Meng Y, Yang R, Tan G, Long Y. Scalable thermochromic smart windows with passive radiative cooling regulation. Science. 2021;374(6574):1501-1504. [DOI][PubMed]
24. Lee D, Choi JS, Kim YJ, Chae YT. Dynamic glazing for a sustainable building future: An in-situ performance evaluation of electrochromic windows in cooling operation. J Build Eng. 2026;120:115574. [DOI]

Publisher's Note

Science Exploration remains a neutral stance on jurisdictional claims in published maps and institutional affiliations. The views expressed in this article are solely those of the author(s) and do not reflect the opinions of the Editors or the publisher.